

Search for Decays of B^0 Mesons into Pairs of Leptons

The *BABAR* Collaboration

July 25, 2002

Abstract

We present a search for the decays $B^0 \rightarrow e^+e^-$, $B^0 \rightarrow \mu^+\mu^-$, and $B^0 \rightarrow e^\pm\mu^\mp$ in data collected at the $\Upsilon(4S)$ with the *BABAR* detector at the SLAC B Factory. Using a data set of 54.4 fb^{-1} , we find no evidence for a signal and set the following preliminary upper limits at the 90% confidence level: $\mathcal{B}(B^0 \rightarrow e^+e^-) < 3.3 \times 10^{-7}$, $\mathcal{B}(B^0 \rightarrow \mu^+\mu^-) < 2.0 \times 10^{-7}$, and $\mathcal{B}(B^0 \rightarrow e^\pm\mu^\mp) < 2.1 \times 10^{-7}$.

Contributed to the 31st International Conference on High Energy Physics,
7/24—7/31/2002, Amsterdam, The Netherlands

Stanford Linear Accelerator Center, Stanford University, Stanford, CA 94309

Work supported in part by Department of Energy contract DE-AC03-76SF00515.

The BABAR Collaboration,

B. Aubert, D. Boutigny, J.-M. Gaillard, A. Hicheur, Y. Karyotakis, J. P. Lees, P. Robbe, V. Tisserand,
A. Zghiche

Laboratoire de Physique des Particules, F-74941 Annecy-le-Vieux, France

A. Palano, A. Pompili

Università di Bari, Dipartimento di Fisica and INFN, I-70126 Bari, Italy

J. C. Chen, N. D. Qi, G. Rong, P. Wang, Y. S. Zhu

Institute of High Energy Physics, Beijing 100039, China

G. Eigen, I. Ofte, B. Stugu

University of Bergen, Inst. of Physics, N-5007 Bergen, Norway

G. S. Abrams, A. W. Borgland, A. B. Breon, D. N. Brown, J. Button-Shafer, R. N. Cahn, E. Charles,
M. S. Gill, A. V. Gritsan, Y. Groysman, R. G. Jacobsen, R. W. Kadel, J. Kadyk, L. T. Kerth,
Yu. G. Kolomensky, J. F. Kral, C. LeClerc, M. E. Levi, G. Lynch, L. M. Mir, P. J. Oddone, T. J. Orimoto,
M. Pripstein, N. A. Roe, A. Romosan, M. T. Ronan, V. G. Shelkov, A. V. Telnov, W. A. Wenzel

Lawrence Berkeley National Laboratory and University of California, Berkeley, CA 94720, USA

T. J. Harrison, C. M. Hawkes, D. J. Knowles, S. W. O'Neale, R. C. Penny, A. T. Watson, N. K. Watson

University of Birmingham, Birmingham, B15 2TT, United Kingdom

T. Deppermann, K. Goetzen, H. Koch, B. Lewandowski, K. Peters, H. Schmuecker, M. Steinke

Ruhr Universität Bochum, Institut für Experimentalphysik 1, D-44780 Bochum, Germany

N. R. Barlow, W. Bhimji, J. T. Boyd, N. Chevalier, P. J. Clark, W. N. Cottingham, C. Mackay,
F. F. Wilson

University of Bristol, Bristol BS8 1TL, United Kingdom

K. Abe, C. Hearty, T. S. Mattison, J. A. McKenna, D. Thiessen

University of British Columbia, Vancouver, BC, Canada V6T 1Z1

S. Jolly, A. K. McKemey

Brunel University, Uxbridge, Middlesex UB8 3PH, United Kingdom

V. E. Blinov, A. D. Bukin, A. R. Buzykaev, V. B. Golubev, V. N. Ivanchenko, A. A. Korol,
E. A. Kravchenko, A. P. Onuchin, S. I. Serebnyakov, Yu. I. Skovpen, A. N. Yushkov

Budker Institute of Nuclear Physics, Novosibirsk 630090, Russia

D. Best, M. Chao, D. Kirkby, A. J. Lankford, M. Mandelkern, S. McMahon, D. P. Stoker

University of California at Irvine, Irvine, CA 92697, USA

C. Buchanan, S. Chun

University of California at Los Angeles, Los Angeles, CA 90024, USA

H. K. Hadavand, E. J. Hill, D. B. MacFarlane, H. Paar, S. Prell, Sh. Rahatlou, G. Raven, U. Schwanke,
V. Sharma

University of California at San Diego, La Jolla, CA 92093, USA

J. W. Berryhill, C. Campagnari, B. Dahmes, P. A. Hart, N. Kuznetsova, S. L. Levy, O. Long, A. Lu,
M. A. Mazur, J. D. Richman, W. Verkerke

University of California at Santa Barbara, Santa Barbara, CA 93106, USA

J. Beringer, A. M. Eisner, M. Grothe, C. A. Heusch, W. S. Lockman, T. Pulliam, T. Schalk, R. E. Schmitz,
B. A. Schumm, A. Seiden, M. Turri, W. Walkowiak, D. C. Williams, M. G. Wilson

University of California at Santa Cruz, Institute for Particle Physics, Santa Cruz, CA 95064, USA

E. Chen, G. P. Dubois-Felsmann, A. Dvoretzki, D. G. Hitlin, F. C. Porter, A. Ryd, A. Samuel, S. Yang
California Institute of Technology, Pasadena, CA 91125, USA

S. Jayatileke, G. Mancinelli, B. T. Meadows, M. D. Sokoloff

University of Cincinnati, Cincinnati, OH 45221, USA

T. Barillari, P. Bloom, W. T. Ford, U. Nauenberg, A. Olivas, P. Rankin, J. Roy, J. G. Smith, W. C. van
Hoek, L. Zhang

University of Colorado, Boulder, CO 80309, USA

J. L. Harton, T. Hu, M. Krishnamurthy, A. Soffer, W. H. Toki, R. J. Wilson, J. Zhang

Colorado State University, Fort Collins, CO 80523, USA

D. Altenburg, T. Brandt, J. Brose, T. Colberg, M. Dickopp, R. S. Dubitzky, A. Hauke, E. Maly,
R. Müller-Pfefferkorn, S. Otto, K. R. Schubert, R. Schwierz, B. Spaan, L. Wilden

Technische Universität Dresden, Institut für Kern- und Teilchenphysik, D-01062 Dresden, Germany

D. Bernard, G. R. Bonneaud, F. Brochard, J. Cohen-Tanugi, S. Ferrag, S. T'Jampens, Ch. Thiebaux,
G. Vasileiadis, M. Verderi

Ecole Polytechnique, LLR, F-91128 Palaiseau, France

A. Anjomshoaa, R. Bernet, A. Khan, D. Lavin, F. Muheim, S. Playfer, J. E. Swain, J. Tinslay

University of Edinburgh, Edinburgh EH9 3JZ, United Kingdom

M. Falbo

Elon University, Elon University, NC 27244-2010, USA

C. Borean, C. Bozzi, L. Piemontese, A. Sarti

Università di Ferrara, Dipartimento di Fisica and INFN, I-44100 Ferrara, Italy

E. Treadwell

Florida A&M University, Tallahassee, FL 32307, USA

F. Anulli,¹ R. Baldini-Ferrolì, A. Calcaterra, R. de Sangro, D. Falciari, G. Finocchiaro, P. Patteri,
I. M. Peruzzi,¹ M. Piccolo, A. Zallo

Laboratori Nazionali di Frascati dell'INFN, I-00044 Frascati, Italy

S. Bagnasco, A. Buzzo, R. Contri, G. Crosetti, M. Lo Vetere, M. Macri, M. R. Monge, S. Passaggio,
F. C. Pastore, C. Patrignani, E. Robutti, A. Santroni, S. Tosi

Università di Genova, Dipartimento di Fisica and INFN, I-16146 Genova, Italy

¹ Also with Università di Perugia, I-06100 Perugia, Italy

S. Bailey, M. Morii

Harvard University, Cambridge, MA 02138, USA

R. Bartoldus, G. J. Grenier, U. Mallik

University of Iowa, Iowa City, IA 52242, USA

J. Cochran, H. B. Crawley, J. Lamsa, W. T. Meyer, E. I. Rosenberg, J. Yi

Iowa State University, Ames, IA 50011-3160, USA

M. Davier, G. Grosdidier, A. Höcker, H. M. Lacker, S. Laplace, F. Le Diberder, V. Lepeltier, A. M. Lutz,
T. C. Petersen, S. Plaszczynski, M. H. Schune, L. Tantot, S. Trincaz-Duvoid, G. Wormser

Laboratoire de l'Accélérateur Linéaire, F-91898 Orsay, France

R. M. Bionta, V. Brigljević, D. J. Lange, K. van Bibber, D. M. Wright

Lawrence Livermore National Laboratory, Livermore, CA 94550, USA

A. J. Bevan, J. R. Fry, E. Gabathuler, R. Gamet, M. George, M. Kay, D. J. Payne, R. J. Sloane,
C. Touramanis

University of Liverpool, Liverpool L69 3BX, United Kingdom

M. L. Aspinwall, D. A. Bowerman, P. D. Dauncey, U. Egede, I. Eschrich, G. W. Morton, J. A. Nash,
P. Sanders, D. Smith, G. P. Taylor

University of London, Imperial College, London, SW7 2BW, United Kingdom

J. J. Back, G. Bellodi, P. Dixon, P. F. Harrison, R. J. L. Potter, H. W. Shorthouse, P. Strother, P. B. Vidal

Queen Mary, University of London, E1 4NS, United Kingdom

G. Cowan, H. U. Flaecher, S. George, M. G. Green, A. Kurup, C. E. Marker, T. R. McMahon, S. Ricciardi,
F. Salvatore, G. Vaitsas, M. A. Winter

University of London, Royal Holloway and Bedford New College, Egham, Surrey TW20 0EX, United Kingdom

D. Brown, C. L. Davis

University of Louisville, Louisville, KY 40292, USA

J. Allison, R. J. Barlow, A. C. Forti, F. Jackson, G. D. Lafferty, A. J. Lyon, N. Savvas, J. H. Weatherall,
J. C. Williams

University of Manchester, Manchester M13 9PL, United Kingdom

A. Farbin, A. Jawahery, V. Lillard, D. A. Roberts, J. R. Schieck

University of Maryland, College Park, MD 20742, USA

G. Blaylock, C. Dallapiccola, K. T. Flood, S. S. Hertzbach, R. Kofler, V. B. Koptchev, T. B. Moore,
H. Staengle, S. Willocq

University of Massachusetts, Amherst, MA 01003, USA

B. Brau, R. Cowan, G. Sciolla, F. Taylor, R. K. Yamamoto

Massachusetts Institute of Technology, Laboratory for Nuclear Science, Cambridge, MA 02139, USA

M. Milek, P. M. Patel

McGill University, Montréal, QC, Canada H3A 2T8

F. Palombo

Università di Milano, Dipartimento di Fisica and INFN, I-20133 Milano, Italy

J. M. Bauer, L. Cremaldi, V. Eschenburg, R. Kroeger, J. Reidy, D. A. Sanders, D. J. Summers

University of Mississippi, University, MS 38677, USA

C. Hast, P. Taras

Université de Montréal, Laboratoire René J. A. Lévesque, Montréal, QC, Canada H3C 3J7

H. Nicholson

Mount Holyoke College, South Hadley, MA 01075, USA

C. Cartaro, N. Cavallo, G. De Nardo, F. Fabozzi, C. Gatto, L. Lista, P. Paolucci, D. Piccolo, C. Sciacca

Università di Napoli Federico II, Dipartimento di Scienze Fisiche and INFN, I-80126, Napoli, Italy

J. M. LoSecco

University of Notre Dame, Notre Dame, IN 46556, USA

J. R. G. Alsmiller, T. A. Gabriel

Oak Ridge National Laboratory, Oak Ridge, TN 37831, USA

J. Brau, R. Frey, M. Iwasaki, C. T. Potter, N. B. Sinev, D. Strom, E. Torrence

University of Oregon, Eugene, OR 97403, USA

F. Colecchia, A. Dorigo, F. Galeazzi, M. Margoni, M. Morandin, M. Posocco, M. Rotondo, F. Simonetto,
R. Stroili, C. Voci

Università di Padova, Dipartimento di Fisica and INFN, I-35131 Padova, Italy

M. Benayoun, H. Briand, J. Chauveau, P. David, Ch. de la Vaissière, L. Del Buono, O. Hamon,
Ph. Leruste, J. Ocariz, M. Pivk, L. Roos, J. Stark

Universités Paris VI et VII, Lab de Physique Nucléaire H. E., F-75252 Paris, France

P. F. Manfredi, V. Re, V. Speziali

Università di Pavia, Dipartimento di Elettronica and INFN, I-27100 Pavia, Italy

L. Gladney, Q. H. Guo, J. Panetta

University of Pennsylvania, Philadelphia, PA 19104, USA

C. Angelini, G. Batignani, S. Bettarini, M. Bondioli, F. Bucci, G. Calderini, E. Campagna, M. Carpinelli,
F. Forti, M. A. Giorgi, A. Lusiani, G. Marchiori, F. Martinez-Vidal, M. Morganti, N. Neri, E. Paoloni,
M. Rama, G. Rizzo, F. Sandrelli, G. Triggiani, J. Walsh

Università di Pisa, Scuola Normale Superiore and INFN, I-56010 Pisa, Italy

M. Haire, D. Judd, K. Paick, L. Turnbull, D. E. Wagoner

Prairie View A&M University, Prairie View, TX 77446, USA

J. Albert, G. Cavoto,² N. Danielson, P. Elmer, C. Lu, V. Miftakov, J. Olsen, S. F. Schaffner,
A. J. S. Smith, A. Tumanov, E. W. Varnes

Princeton University, Princeton, NJ 08544, USA

² Also with Università di Roma La Sapienza, Roma, Italy

F. Bellini, D. del Re, R. Faccini,³ F. Ferrarotto, F. Ferroni, E. Leonardi, M. A. Mazzone, S. Morganti,
G. Piredda, F. Safai Tehrani, M. Serra, C. Voena

Università di Roma La Sapienza, Dipartimento di Fisica and INFN, I-00185 Roma, Italy

S. Christ, G. Wagner, R. Waldi

Universität Rostock, D-18051 Rostock, Germany

T. Adye, N. De Groot, B. Franek, N. I. Geddes, G. P. Gopal, S. M. Xella

Rutherford Appleton Laboratory, Chilton, Didcot, Oxon, OX11 0QX, United Kingdom

R. Aleksan, S. Emery, A. Gaidot, P.-F. Giraud, G. Hamel de Monchenault, W. Kozanecki, M. Langer,
G. W. London, B. Mayer, G. Schott, B. Serfass, G. Vasseur, Ch. Yeche, M. Zito

DAPNIA, Commissariat à l'Energie Atomique/Saclay, F-91191 Gif-sur-Yvette, France

M. V. Purohit, A. W. Weidemann, F. X. Yumiceva

University of South Carolina, Columbia, SC 29208, USA

I. Adam, D. Aston, N. Berger, A. M. Boyarski, M. R. Convery, D. P. Coupal, D. Dong, J. Dorfan,
W. Dunwoodie, R. C. Field, T. Glanzman, S. J. Gowdy, E. Grauges, T. Haas, T. Hadig, V. Halyo,
T. Himel, T. Hryn'ova, M. E. Huffer, W. R. Innes, C. P. Jessop, M. H. Kelsey, P. Kim, M. L. Kocian,
U. Langenegger, D. W. G. S. Leith, S. Luitz, V. Luth, H. L. Lynch, H. Marsiske, S. Menke, R. Messner,
D. R. Muller, C. P. O'Grady, V. E. Ozcan, A. Perazzo, M. Perl, S. Petrak, H. Quinn, B. N. Ratcliff,
S. H. Robertson, A. Roodman, A. A. Salnikov, T. Schietinger, R. H. Schindler, J. Schwiening, G. Simi,
A. Snyder, A. Soha, S. M. Spanier, J. Stelzer, D. Su, M. K. Sullivan, H. A. Tanaka, J. Va'vra,
S. R. Wagner, M. Weaver, A. J. R. Weinstein, W. J. Wisniewski, D. H. Wright, C. C. Young

Stanford Linear Accelerator Center, Stanford, CA 94309, USA

P. R. Burchat, C. H. Cheng, T. I. Meyer, C. Roat

Stanford University, Stanford, CA 94305-4060, USA

R. Henderson

TRIUMF, Vancouver, BC, Canada V6T 2A3

W. Bugg, H. Cohn

University of Tennessee, Knoxville, TN 37996, USA

J. M. Izen, I. Kitayama, X. C. Lou

University of Texas at Dallas, Richardson, TX 75083, USA

F. Bianchi, M. Bona, D. Gamba

Università di Torino, Dipartimento di Fisica Sperimentale and INFN, I-10125 Torino, Italy

L. Bosisio, G. Della Ricca, S. Dittongo, L. Lanceri, P. Poropat, L. Vitale, G. Vuagnin

Università di Trieste, Dipartimento di Fisica and INFN, I-34127 Trieste, Italy

R. S. Panvini

Vanderbilt University, Nashville, TN 37235, USA

³ Also with University of California at San Diego, La Jolla, CA 92093, USA

S. W. Banerjee, C. M. Brown, D. Fortin, P. D. Jackson, R. Kowalewski, J. M. Roney

University of Victoria, Victoria, BC, Canada V8W 3P6

H. R. Band, S. Dasu, M. Datta, A. M. Eichenbaum, H. Hu, J. R. Johnson, R. Liu, F. Di Lodovico,
A. Mohapatra, Y. Pan, R. Prepost, I. J. Scott, S. J. Sekula, J. H. von Wimmersperg-Toeller, J. Wu,
S. L. Wu, Z. Yu

University of Wisconsin, Madison, WI 53706, USA

H. Neal

Yale University, New Haven, CT 06511, USA

1 Introduction

In the Standard Model (SM), rare B decays such as $B^0 \rightarrow \ell^+ \ell^-$, where ℓ refers to e, μ , are expected to proceed through box and loop diagrams as shown in Fig. 1. These decays are highly suppressed

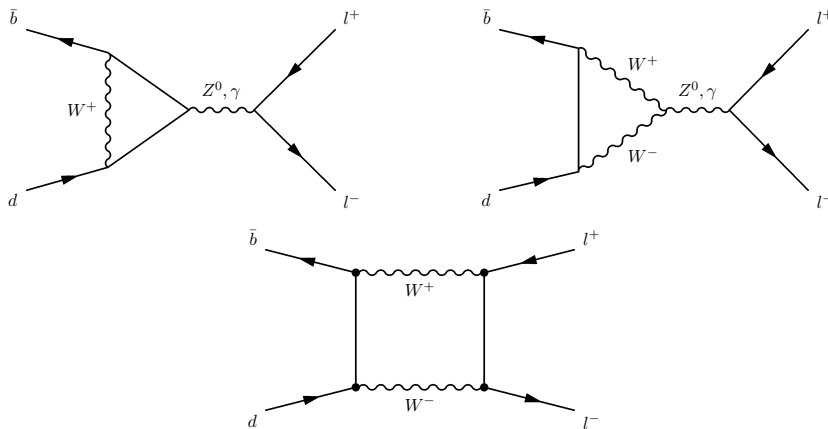


Figure 1: Feynman diagrams for $B^0 \rightarrow \ell^+ \ell^-$ in the Standard Model.

since they involve a $b \rightarrow d$ transition and require an internal quark annihilation within the B meson which further suppresses the decay by a factor of $(f_B/M_B)^2 \approx 2 \times 10^{-3}$ relative to the electroweak “penguin” $b \rightarrow d\gamma$ decay. In addition, the decays are helicity suppressed by factors of $(m_\ell/m_B)^2$. B^0 decays to leptons of two different flavors, $B^0 \rightarrow e^\pm \mu^\mp$, violate lepton flavor conservation and are therefore strictly forbidden in the SM, although permitted in extensions to the SM with non-zero neutrino mass [1]. The $B^0 \rightarrow e^\pm \mu^\mp$ channel includes both $B^0 \rightarrow e^+ \mu^-$ and $B^0 \rightarrow e^- \mu^+$. To date, $B^0 \rightarrow \ell^+ \ell^-$ decays have not been observed. The current best limits from the CLEO [2] and Belle [3] collaborations are compared with the SM expectations in Table 1.

$B^0 \rightarrow \ell^+ \ell^-$ decays involving tau leptons involve either a soft electron, muon, or meson and missing energy (from one or more neutrinos), and require a rather different search strategy than that presented here for the $B^0 \rightarrow e^+ e^-$, $B^0 \rightarrow \mu^+ \mu^-$, and $B^0 \rightarrow e^\pm \mu^\mp$ channels. The presence of the soft electron or muon in the tau channels eliminates them as a source of background to the non-tau channels.

Since these processes are highly suppressed in the SM, they are potentially sensitive probes of physics beyond the SM. Although the branching ratios for these processes are not significantly enhanced in the Minimal Supersymmetric Standard Model (MSSM), various non-minimal supersymmetric models predict branching ratios that are significantly larger than those of the SM. Also, multi-Higgs-doublet models with natural flavor conservation have extra charged Higgs particles which replace the SM W -boson in the box diagram of Fig. 1 and may enhance the $B^0 \rightarrow \ell^+ \ell^-$ branching ratios by an order of magnitude [4]. Similarly, in models with an extra vector-like down-type quark [5], flavor changing neutral currents (FCNC) involving the Z^0 boson are induced due to the different isospin charge of the exotic quark. These models predict the rate for $B^0 \rightarrow \ell^+ \ell^-$ to be about two orders of magnitude larger than the expected SM rate [6]. In addition, $B^0 \rightarrow \ell^+ \ell^-$ decays are allowed in specific models containing leptoquarks [7] and supersymmetric (SUSY) models without R -parity conservation. Furthermore, flavor violating channels such as $B^0 \rightarrow e^\pm \mu^\mp$ could be enhanced by leptoquarks or R -parity violating operators in SUSY models.

As shown in Table 1, sensitivity even to models which produce an enhancement of a few orders of magnitude to the SM rates for these rare decays is beyond current experimental capabilities. Observation of a $B^0 \rightarrow \ell^+ \ell^-$ decay would, in consequence, provide clear evidence for physics beyond the Standard Model.

Table 1: The expected branching ratios in the Standard Model [8] and the current best upper limits (U.L.) in units of 10^{-7} at the 90% C.L. from CLEO [2] and Belle [3]. In addition, the measured number of events N_{obs} in the signal region, the expected background in the signal region $N_{\text{exp}}^{\text{bg}}$, and the reconstruction efficiency ε are quoted. CLEO’s analysis was performed on a data set corresponding to 9.1 fb^{-1} , Belle’s measurement was performed on a data set of 21.3 fb^{-1} .

Decay Mode	SM Expect.	CLEO				Belle			
		U.L.	N_{obs}	$N_{\text{exp}}^{\text{bg}}$	$\varepsilon[\%]$	U.L.	N_{obs}	$N_{\text{exp}}^{\text{bg}}$	$\varepsilon[\%]$
e^+e^-	1.9×10^{-15}	8.3	0	0.11 ± 0.07	$31.1 \pm 0.4 \pm 2.4$	6.3	1	0.6 ± 0.8	31.3 ± 2.4
$\mu^+\mu^-$	8.0×10^{-11}	6.1	0	0.22 ± 0.07	$42.4 \pm 0.5 \pm 3.2$	2.8	0	0.7 ± 0.8	40.0 ± 4.3
$e^\pm\mu^\mp$	–	15	2	0.49 ± 0.20	$43.6 \pm 0.5 \pm 7.1$	9.4	3	0.7 ± 0.8	35.8 ± 3.2

2 The *BABAR* detector and dataset

The data used in these analyses were collected with the *BABAR* detector at the PEP-II e^+e^- storage ring during the years 2000 and 2001. The sample corresponds to an integrated luminosity of 54.4 fb^{-1} accumulated on the $\Upsilon(4S)$ resonance (“on-resonance”) and 6.4 fb^{-1} accumulated at a center-of-mass (CM) energy about 40 MeV below the $\Upsilon(4S)$ resonance (“off-resonance”), which are used for the non-resonant $q\bar{q}$ background studies. The on-resonance sample corresponds to $(59.9 \pm 0.7) \times 10^6 B\bar{B}$ pairs. The collider is operated with asymmetric beam energies, producing a boost ($\beta\gamma = 0.55$) of the $\Upsilon(4S)$ along the collision axis.

BABAR is a solenoidal detector optimized for the asymmetric beam configuration at PEP-II and is described in detail in Ref. [9]. The 1.5 T superconducting magnet, whose cylindrical volume is 1.4 m in radius and 3 m long, contains a charged-particle tracking system, a Cherenkov detector (DIRC) dedicated to charged particle identification, and a central electromagnetic calorimeter consisting of 5760 CsI(Tl) crystals. A forward endcap electromagnetic calorimeter consists of 820 CsI(Tl) crystals. The segmented flux return, including endcaps, is instrumented with resistive plate chambers for muon and K_L^0 identification. This subsystem is referred to as the instrumented flux return (IFR). The tracking system consists of a 5-layer double-sided silicon vertex tracker and a 40-layer drift chamber filled with a gas mixture of helium and isobutane.

3 Analysis method

The presence of two charged high-momentum leptons provides for a very clean signature for the three decay modes under consideration. In the CM we require two oppositely-charged high-momentum leptons (*i.e.* $|p_\ell| \sim m_B/2$) from a common vertex consistent with the decay of a B^0 meson¹. Since the signal events contain two B^0 mesons and no additional particles, the energy of

¹Charge-conjugation is implied throughout this paper.

each B^0 in the CM frame must be equal to the e^+ or e^- beam energy. We therefore define

$$m_{ES} = \sqrt{(E_{\text{beam}}^*)^2 - (\sum_i \mathbf{p}_i^*)^2} \quad (1)$$

$$\Delta E = \sum_i \sqrt{m_i^2 + (\mathbf{p}_i^*)^2} - E_{\text{beam}}^*, \quad (2)$$

where E_{beam}^* is the beam energy in the $\Upsilon(4S)$ CM frame, \mathbf{p}_i^* is the CM momentum of particle i in the candidate B^0 -meson system, and m_i is the mass of particle i . For signal events, the beam-energy-substituted B^0 mass, m_{ES} , peaks at m_B . The quantity ΔE is used to determine whether a candidate system of particles has total energy consistent with the beam energy in the CM frame. We require that the beam-energy substituted mass, m_{ES} , be very close to the mass of the B^0 meson and that ΔE be close to zero [9].

To remove background from lepton misidentification, we require tight electron and muon identification criteria. The electron identification relies on E/p , the ratio of energy deposited in the calorimeter to the momentum of the particle at the origin, the lateral and azimuthal shower profiles, and the consistency of DIRC Cherenkov angle with an electron hypothesis. The muon identification relies on the total number of hits in the IFR, the distribution of hits in the different layers, the amount of energy released in the calorimeter, and the number of interaction lengths which the track has traversed. Suppression of background from non-resonant $q\bar{q}$ production is provided by a series of topological requirements. In particular, we employ restrictions on the overall magnitude of the event thrust and on the magnitude of the cosine of the thrust angle, θ_T , defined as the angle between the thrust axis of the particles that form the reconstructed B^0 candidate and the thrust axis of the remaining tracks and neutral clusters in the event. We also cut on the total multiplicity of both charged tracks and neutral particles by means of the variable N_{mult} defined as

$$N_{\text{mult}} = N_{\text{trk}} + \frac{1}{2}N_{\gamma}, \quad (3)$$

where N_{trk} is the total number of tracks in the event and N_{γ} is the number of photons found with an energy $E_{\gamma} > 80$ MeV. We require $N_{\text{mult}} \geq 6.0$. This variable is especially useful in the rejection of radiative Bhabha events. We also require that the total energy in the event be less than 11 GeV. This cut is effective in reducing background from two photon events.

$B^0 \rightarrow \ell^+\ell^-$ candidates are selected by simultaneous requirements on the energy difference ΔE and the energy-substituted mass m_{ES} . The size of this “signal box” is chosen to be roughly $[+2, -2]\sigma$ of the expected resolution in ΔE and $[+2, -2]\sigma$ for m_{ES} , optimized for the best upper limit. In the cases of the $B^0 \rightarrow e^+e^-$ and $B^0 \rightarrow e^{\pm}\mu^{\mp}$ decay modes, the signal box sizes in ΔE are relaxed to roughly $[+2, -3]\sigma$ and $[+2, -2.5]\sigma$, respectively, to accommodate a tail in the distribution resulting from final state radiation and bremsstrahlung. Table 3 gives the m_{ES} and ΔE resolutions for the three signal channels. Figure 2 illustrates the m_{ES} and ΔE distributions for Monte Carlo (MC) signal events. For the ΔE distribution, the tail due to final state radiation and bremsstrahlung is well described by a “Novosibirsk” function [10]. Table 2 summarizes the m_{ES} and ΔE cut values used to define the different boxes in the $(\Delta E, m_{ES})$ plane.

We also chose to optimize the cuts on the magnitude of the overall event thrust $|T|$ and $|\cos\theta_T|$ simultaneously (due to the large correlation). The optimal selection criteria for all three channels was found to be $|\cos\theta_T| < 0.84$ and $|T| < 0.9$. Figure 3 illustrates the distributions of the multiplicity and event shape variables in signal and background MC, which are dominated by non-resonant $c\bar{c}$ - and uds -continuum processes, but also include small components from $b\bar{b}$ and

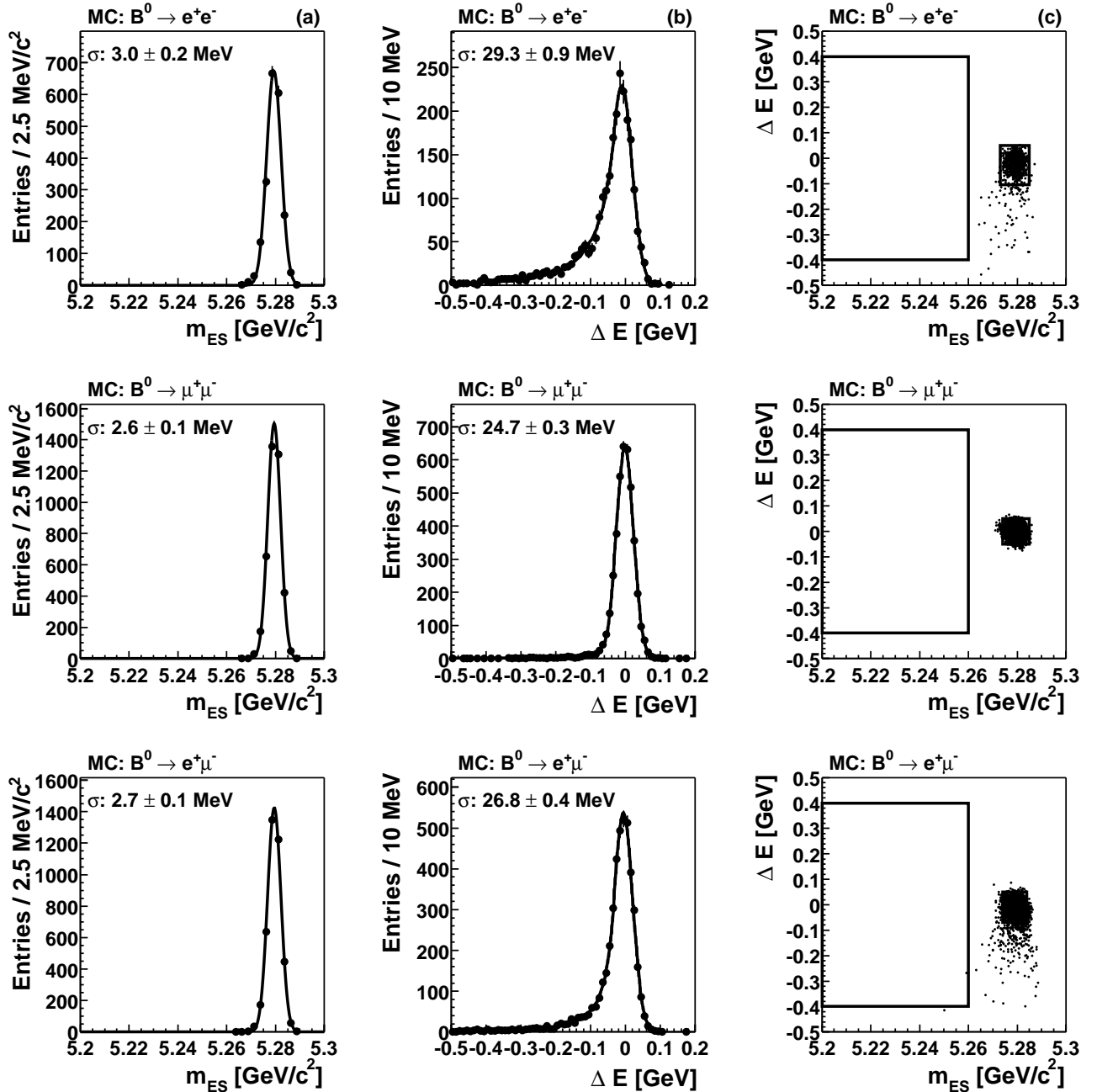


Figure 2: Reconstruction of B meson candidates in $B^0 \rightarrow e^+e^-$ MC (top row), $B^0 \rightarrow \mu^+\mu^-$ MC (middle row), and $B^0 \rightarrow e^+\mu^-$ MC (bottom row) with the beam-energy substituted mass m_{ES} (a) and ΔE , the difference between the beam energy and the energy of the B -meson candidate in the CM frame (b). A “Novosibirsk” function [10] is used to obtain the widths of the core distribution. Figures (c) show the distribution of ΔE vs m_{ES} . The smaller box on the right defines the signal box. The tail visible on the lower side of the signal box is due to final state radiation and bremsstrahlung. The larger box defines the Grand Sideband (GSB) region.

Table 2: Definition of the signal and Grand Sideband boxes in the $(\Delta E, m_{ES})$ plane. The units for m_{ES} are $[\text{GeV}/c^2]$ and the units for ΔE are $[\text{GeV}]$.

Box Name	$B^0 \rightarrow e^+e^-$		$B^0 \rightarrow \mu^+\mu^-$		$B^0 \rightarrow e^\pm\mu^\mp$	
	m_{ES}	ΔE	m_{ES}	ΔE	m_{ES}	ΔE
Signal Box	5.273–5.285	-0.105–0.050	5.274–5.285	-0.050–0.050	5.274–5.284	-0.070–0.050
Grand Sideband	5.200–5.260	-0.400–0.400	5.200–5.260	-0.400–0.400	5.200–5.260	-0.400–0.400

τ events. All selection criteria have been applied except for the cut on the variable illustrated. The efficiencies of the full selection are given in Table 4. The systematic error on the efficiency is determined by a comparison of the control sample $B^0 \rightarrow J/\psi K_S^0$, with $J/\psi \rightarrow e^+e^-$ for $B^0 \rightarrow e^+e^-$ and $J/\psi \rightarrow \mu^+\mu^-$ for $B^0 \rightarrow \mu^+\mu^-$, respectively in data and MC simulation. These comparisons found the dominant uncertainty on the signal efficiency to be the resolution and scale of ΔE , contributing 4.4% and 2.6% for the $B^0 \rightarrow e^+e^-$ and $B^0 \rightarrow \mu^+\mu^-$ channels respectively. Since there is no appropriate control sample for the $B^0 \rightarrow e^\pm\mu^\mp$ channel, we conservatively set it to be equal to the largest error obtained from the systematic study for the other channels. This yields systematic errors for all of the main cuts except the multiplicity cut. The systematic error associated with the remaining cuts is determined with a comparison of signal MC samples based on GEANT3 [11] and GEANT4 [12]. These two simulations employ different material models where the latter is considered to be more accurate.

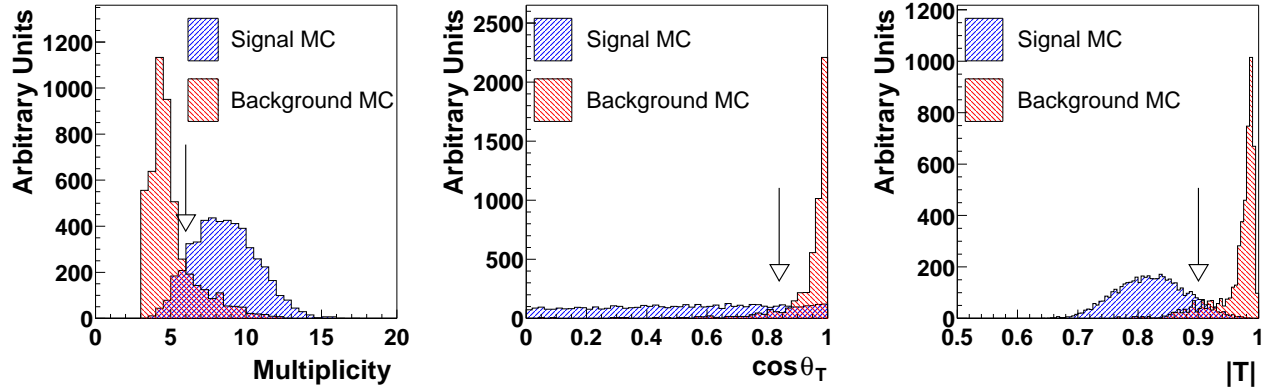


Figure 3: Distributions of the main cuts in signal MC and background MC. The histograms are normalized to equal area. The cut values are indicated by arrows. The composition of the background MC is explained in the text.

Table 3: m_{ES} and ΔE resolutions for the three signal channels.

	$B^0 \rightarrow e^+e^-$	$B^0 \rightarrow \mu^+\mu^-$	$B^0 \rightarrow e^\pm\mu^\mp$
$\sigma(m_{ES})$ $[\text{MeV}/c^2]$	3.0 ± 0.2	2.6 ± 0.1	2.7 ± 0.1
$\sigma(\Delta E)$ $[\text{MeV}]$	29.3 ± 0.9	24.7 ± 0.3	26.8 ± 0.4

We estimate the background level in the signal box from the data. The background expectation

is dominated by different sources in the three channels. For the $B^0 \rightarrow e^+e^-$ channel, the background expectation is dominated by pairs of true electrons from $c\bar{c}$ events and two-photon events. For the $B^0 \rightarrow \mu^+\mu^-$ channel, about 50% of the total background is due to misidentified hadrons (in combination with a real muon). Two-photon processes do not contribute to the background for this channel. For the $B^0 \rightarrow e^\pm\mu^\mp$ channel, the background is composed of real electrons and fake muons. Two-photon processes contribute strongly to the background.

To compare background distributions in data and Monte Carlo event samples, we use the ‘‘Grand Sideband’’ (GSB) box as defined in Table 2. This box is also used to estimate the functional behavior of the ΔE dependence of the background.

We estimate the background in the signal box assuming that it is described by the ARGUS function [13] in m_{ES} and an exponential function in ΔE . The shape parameters of the functions are determined in two different ways: from fitting the data sidebands and from fitting a high statistics fast Monte Carlo $c\bar{c}$ sample. In both cases, we determine the normalization in the grand sideband and derive the number, N_{sigBox} , of expected background as follows:

$$N_{\text{sigBox}} = \frac{\int_{\text{sigBox}} f(m_{ES}) dm_{ES}}{\int_{\text{GSB}} f(m_{ES}) dm_{ES}} \times \frac{\int_{\text{sigBox}} g(\Delta E) d(\Delta E)}{\int_{\text{GSB}} g(\Delta E) d(\Delta E)} \times N_{\text{GSB}} \quad (4)$$

where N_{GSB} is the number of background events found in the GSB, and f and g are the shapes as determined by the ARGUS and exponential fits. The total background expectations for the three channels are given in Table 4.

The actual contents of the signal box were not revealed until the selection criteria and systematic error estimates were frozen. This technique, often referred to as a *blind* analysis, is adopted to avoid possible experimenter bias.

4 Results

When the contents of the signal box were revealed, one event was found in the $B^0 \rightarrow e^+e^-$ channel and no events were found in the other channels as summarized in Table 4. The $(m_{ES}, \Delta E)$ distributions from data for the three channels are shown in Fig. 4. As can be seen from Table 4, the number of events found in the signal box are compatible with the expected background.

We do not perform background subtraction for the determination of the upper limit of the branching fraction. Not yet accounting for the systematic uncertainties, the upper limit on the branching fraction $\mathcal{B}_{\text{UL}}(\text{stat})$ is calculated as $\mathcal{B}_{\text{UL}}(\text{stat}) = N_{\text{UL}}/S = N_{\text{UL}}/(\varepsilon \times (N_{B^0} + N_{\bar{B}^0}))$, where N_{UL} is the upper limit on the number of observed events N_{obs} and S is the sensitivity. $N_{B^0} + N_{\bar{B}^0}$ is equal to the number of $\Upsilon(4S)$ decays, since we assume equal production of B^+ and B^0 in $\Upsilon(4S)$ decays.

In order to include our systematic uncertainty in the determination of the upper limit, we follow the prescription given in Ref. [14]. Assuming a normal distribution for the uncertainty in $1/S$, the systematic uncertainty is accounted for by convolving the Poisson probability distribution for the assumed branching fraction with a Gaussian error distribution for $1/S$. The systematic uncertainty on the signal efficiency is found to be 8.2% for the $B^0 \rightarrow e^+e^-$ channel, where the main contribution comes from the modeling of the m_{ES} and ΔE resolutions, and from the uncertainty in the efficiency of the multiplicity N_{mult} requirement. For the $B^0 \rightarrow \mu^+\mu^-$ channel, the systematic uncertainty on the signal efficiency was found to be 4.7%, with the primary contribution again being from the modeling of the m_{ES} and ΔE resolutions. For the $B^0 \rightarrow e^\pm\mu^\mp$ channel, the systematic uncertainty on the signal efficiency was taken to be the same as for the $B^0 \rightarrow e^+e^-$ channel. The total

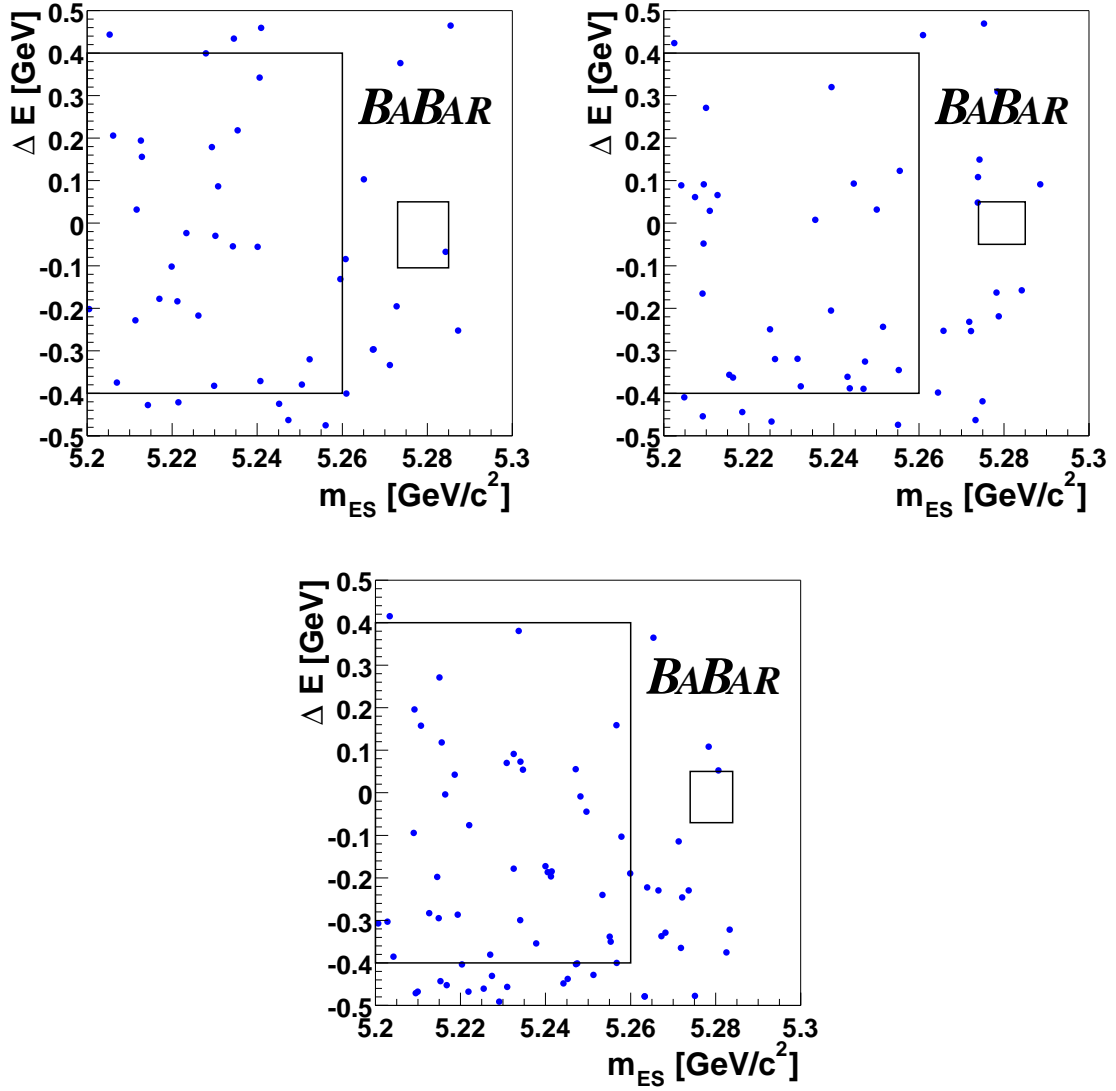


Figure 4: Distributions from data of m_{ES} vs ΔE for $B^0 \rightarrow e^+e^-$ (top left), $B^0 \rightarrow \mu^+\mu^-$ (top right), and $B^0 \rightarrow e^\pm\mu^\mp$ (bottom).

Table 4: Summary of the analyses. N_{exp} is the number of expected signal events, assuming a branching fraction of 1.9×10^{-15} for the $B^0 \rightarrow e^+e^-$ channel and 8.0×10^{-11} for the $B^0 \rightarrow \mu^+\mu^-$ channel. N_{obs} is the number of observed events in the signal box. $N_{\text{exp}}^{\text{bg}}$ is the expected number of background events in the signal box. $\mathcal{B}_{\text{UL}}(B^0 \rightarrow \ell^+\ell^-)$ is the upper limit on the branching ratio at the 90% C.L.

channel	N_{exp}	N_{obs}	$N_{\text{exp}}^{\text{bg}}$	$\varepsilon[\%]$	$\mathcal{B}_{\text{UL}}(B^0 \rightarrow \ell^+\ell^-)$
$B^0 \rightarrow e^+e^-$	1.9×10^{-8}	1	0.60 ± 0.24	$19.3 \pm 0.4_{\text{stat}} \pm 1.6_{\text{sys}}$	3.3×10^{-7}
$B^0 \rightarrow \mu^+\mu^-$	3.2×10^{-2}	0	0.49 ± 0.19	$18.8 \pm 0.3_{\text{stat}} \pm 2.0_{\text{sys}}$	2.0×10^{-7}
$B^0 \rightarrow e^\pm\mu^\mp$	–	0	0.51 ± 0.17	$18.3 \pm 0.4_{\text{stat}} \pm 1.5_{\text{sys}}$	2.1×10^{-7}

uncertainty was calculated by summing in quadrature the systematic uncertainty on the number of $B\bar{B}$ events, the signal efficiency, and the statistical error on the signal efficiency.

As summarized in Table 4, the resulting preliminary upper limits for $\mathcal{B}(B^0 \rightarrow e^+e^-)$, $\mathcal{B}(B^0 \rightarrow \mu^+\mu^-)$, and $\mathcal{B}(B^0 \rightarrow e^\pm\mu^\mp)$ are 3.3×10^{-7} , 2.0×10^{-7} , and 2.1×10^{-7} respectively.

5 Acknowledgments

We are grateful for the extraordinary contributions of our PEP-II colleagues in achieving the excellent luminosity and machine conditions that have made this work possible. The success of this project also relies critically on the expertise and dedication of the computing organizations that support *BABAR*. The collaborating institutions wish to thank SLAC for its support and the kind hospitality extended to them. This work is supported by the US Department of Energy and National Science Foundation, the Natural Sciences and Engineering Research Council (Canada), Institute of High Energy Physics (China), the Commissariat à l’Energie Atomique and Institut National de Physique Nucléaire et de Physique des Particules (France), the Bundesministerium für Bildung und Forschung and Deutsche Forschungsgemeinschaft (Germany), the Istituto Nazionale di Fisica Nucleare (Italy), the Research Council of Norway, the Ministry of Science and Technology of the Russian Federation, and the Particle Physics and Astronomy Research Council (United Kingdom). Individuals have received support from the A. P. Sloan Foundation, the Research Corporation, and the Alexander von Humboldt Foundation.

References

- [1] M. Maki, M. Nakagawa, and S. Sakata, Prog. Theor. Phys. **28**, 870 (1962); V.N. Gribov and B. Pontecorvo, Phys. Lett. **B28**, 493 (1969).
- [2] CLEO Collaboration, T. Bergfeld *et al.*, Phys. Rev. D**62**, 091102(R) (2000).
- [3] Belle Collaboration, K. Abe *et al.*, BELLE-CONF-0127 (2001), KEK-PREPRINT-2001-88.
- [4] See, for example, J.L. Hewett, S. Nandi, and T.G. Rizzo, Phys. Rev. D**39**, 250 (1989); X.G. He, T.D. Nguyen, and R.R. Volkas, Phys. Rev D**38**, 814 (1988); H.E. Logan and U. Nierste, hep-ph/0004139, FERMILAB-Pub-00/084-T.
- [5] Y. Nir and D. Silverman, Phys. Rev. D**42**, 1477 (1990).

- [6] M. Gronau and D. London, Phys. Rev. D**55**, 2845 (1997).
- [7] J. Pati and A. Salam, Phys. Rev. D**10**, 275 (1974).
- [8] A. Ali, C. Greub, and T. Mannel, in *Proceedings of the ECFA Workshop on the Physics of the European B Meson Factory*, edited by R. Aleksan and A. Ali, p. 155 (ECFA-93-151,C93/03/26).
- [9] BABAR Collaboration, B. Aubert *et al.*, Nucl. Instrum. and Methods A **479**, 1 (2002).
- [10] BABAR defines the Novosibirsk function to be
- $$f(E) = A \cdot \exp \left[-\frac{1}{2} \left(\frac{\log(1+\tau(E-\nu) \cdot \frac{\sinh(\tau\sqrt{\log 4})}{\sigma\tau\sqrt{\log 4}})}{\tau} \right)^2 + \tau^2 \right],$$
- where τ is the “tail parameter” (describing how much is contained in the tail), σ is the width, and ν is the peak position.
- [11] R. Brun *et al.*, GEANT *Detector Description and Simulation Tool*, 1993, CERN Program Library Number Q123.
- [12] GEANT4 collaboration, *GEANT4 - a simulation toolkit*, submitted to Nucl. Instrum. and Methods A, CERN-IT-2002-003.
- [13] ARGUS Collaboration, H. Albrecht *et al.*, Phys. Lett. B **241**, 278 (1990);
The ARGUS distribution is described by the following
- $$\frac{dN}{dm_{ES}} \propto m_{ES} \times \sqrt{1 - \frac{m_{ES}^2}{E_{\text{beam}}^{*2}}} \times \exp \left[-\zeta \left(1 - \frac{m_{ES}^2}{E_{\text{beam}}^{*2}} \right) \right];$$
- [14] R.D. Cousins and V.L. Highland, Nucl. Instrum. and Methods A **320**, 331 (1992).